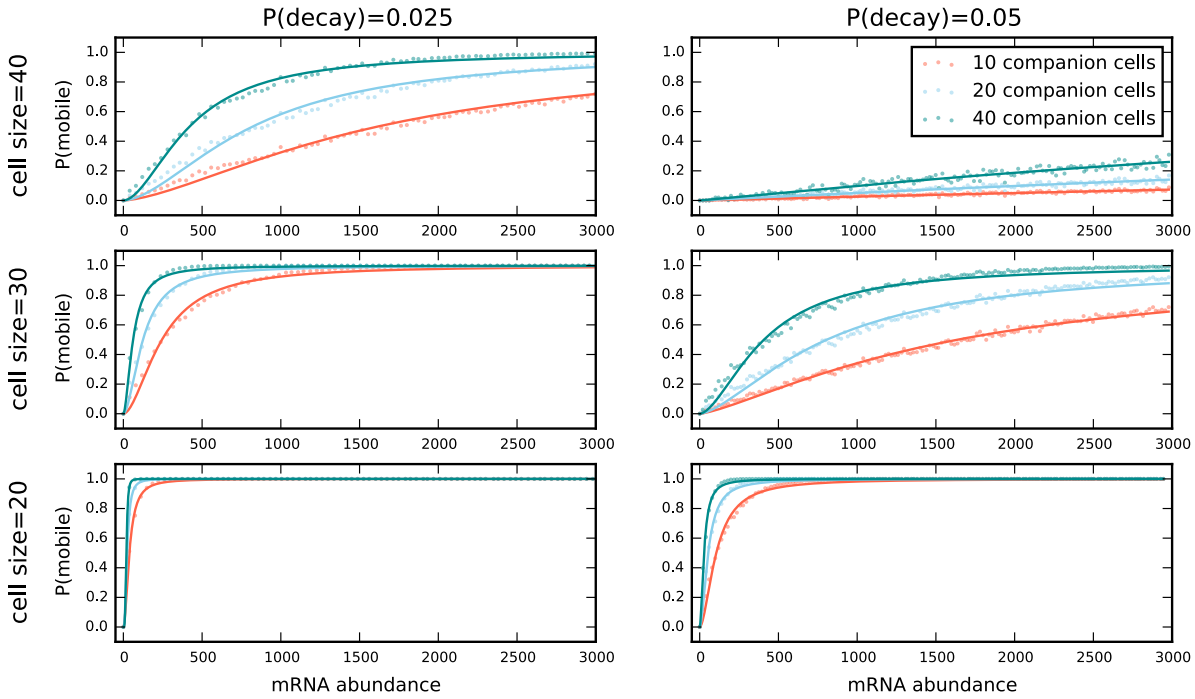


**Supplemental Figure 1: The effect of cell size, cell number and half-life on mRNA mobility.** The mRNA abundance model predictions for the effect of species abundance on mRNA mobility, and the saturation curve approximations of these are shown for simulations with varied cell size, cell number, and mRNA half-life characterized by the probability of decay, P(decay). Points are model predictions based on the calculation of the escape probability from a companion cell in the 3D cell simulations described in the main text. The curves correspond to a fitted saturation equation for a transcript being mobile as explained in the Methods section. This shows that although these unknown parameters all influence mobility, the effects can be well approximated by a simple saturation curve, thus reducing the number of unknown parameters in the model.

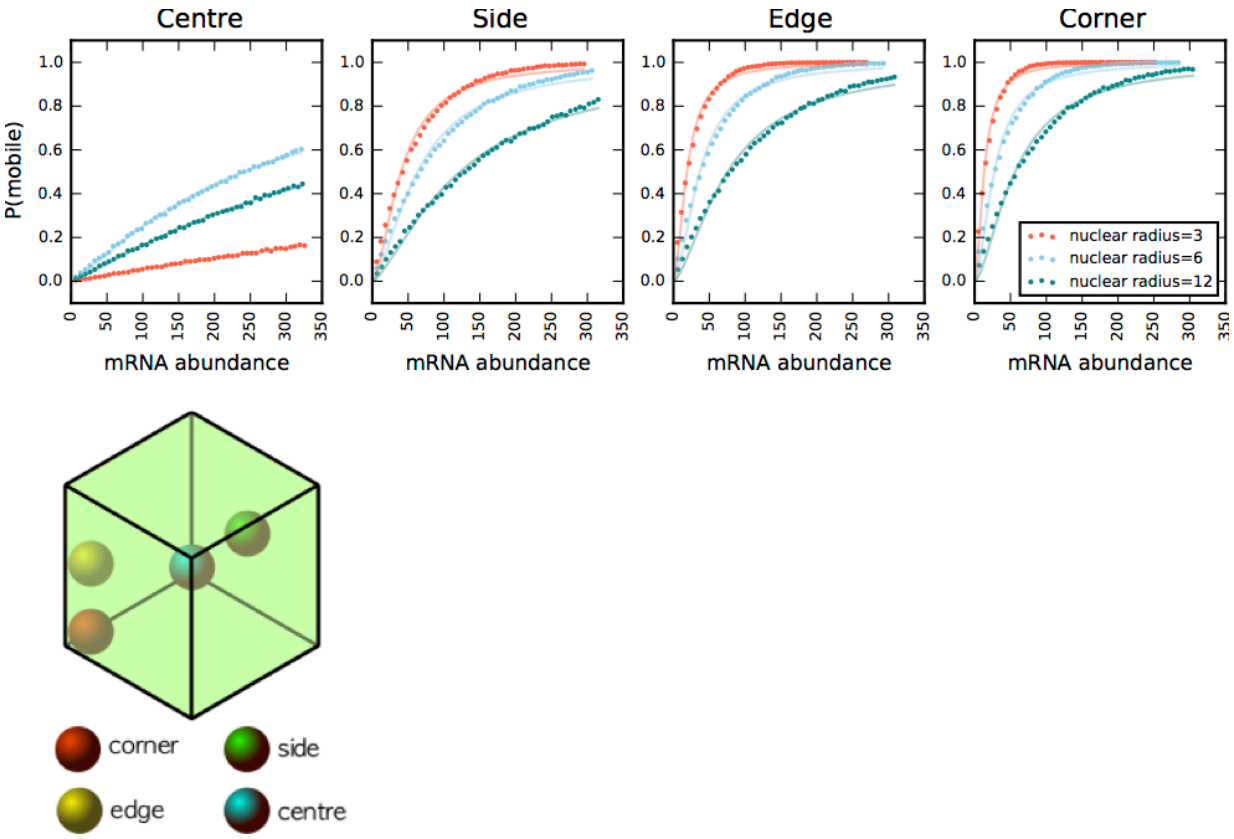


**Supplemental Figure 2: The effect of nucleus position and size on mRNA mobility.** The abundance model predictions for the effect of species abundance on mRNA mobility and the saturation curve approximations of these are shown for simulations with varied nucleus position and size. Variation in nucleus size and position was incorporated in the abundance model by modifying the initial position of the simulated mRNA molecule. Starting positions were uniformly sampled on the surface of a sphere, representing the nucleus, positioned as shown, and of stated radius. Points are model predictions based on the calculation of the escape probability from a companion cell in the 3D cell simulations described in the main text. The curves correspond to a fitted saturation equation for a transcript being mobile as explained in the Methods section. This shows that although these unknown parameters all influence mobility, the effects can be well approximated by a simple saturation curve, thus reducing the number of unknown parameters in the model.

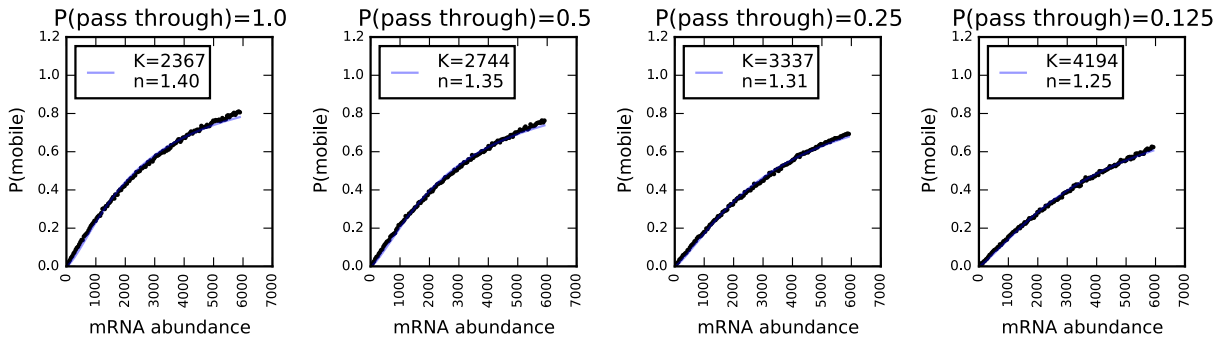


**Supplemental Figure 3: The effect of varied probability of passing through the cell surface on mRNA mobility.** The abundance model predictions for the effect of species abundance on mRNA mobility and the saturation curve approximations of these are shown for simulations with varied probability of passing through the cell surface upon contact with it. With decreased probability of passing through the surface, K was seen to increase, and n decrease. Points are model predictions based on the calculation of the escape probability from a companion cell in the 3D cell simulations described in the main text. The curves correspond to a fitted saturation equation for a transcript being mobile as explained in the Methods section. This shows that although these unknown parameters all influence mobility, the effects can be well approximated by a simple saturation curve, thus reducing the number of unknown parameters in the model.

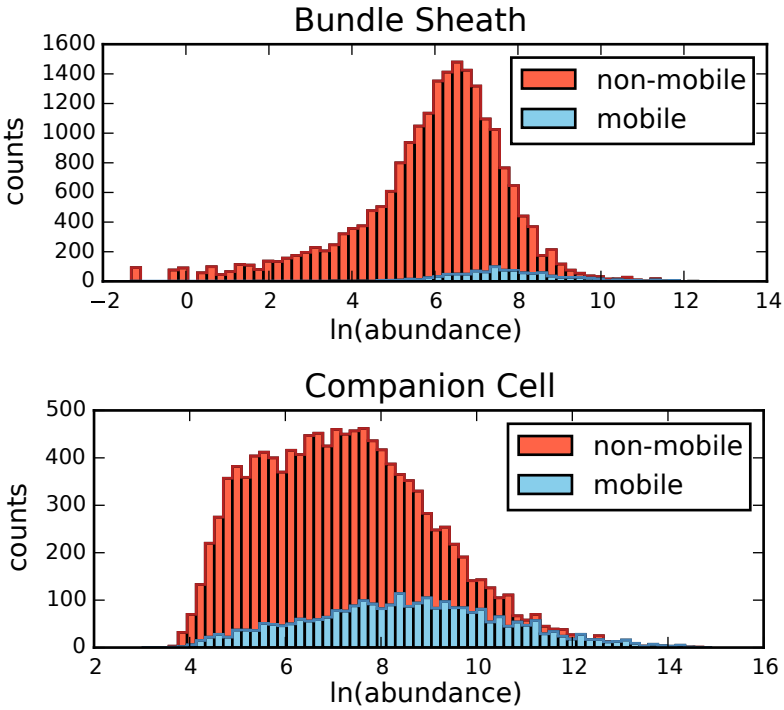


**Supplemental Figure 4: The abundance distribution of mobile and non-mobile transcripts in cells proximal to the vasculature.** Abundance data for the bundle sheath from Aubry et al. (2014), for the companion cell from Mustroph et al. (2009), mobility classification data from Thieme et al. (2015).

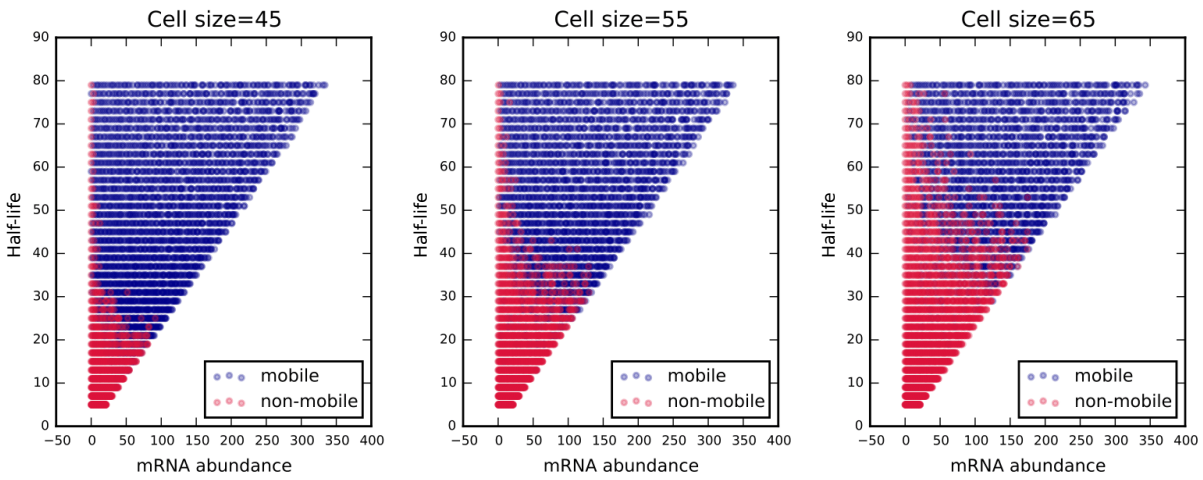


**Supplemental Figure 5: The predicted effect of half-life and abundance on transcript mobility.** For varied transcription rates and half-lives, transcript abundance and mobility was simulated using the abundance cell model. Transcripts with longer half-lives can be seen to be more mobile than shorter transcripts. However, the effect of half-life on mobility can be seen to interact with transcript abundance, such that the threshold half-life, and sensitivity to changes in half-life varies with species abundance.

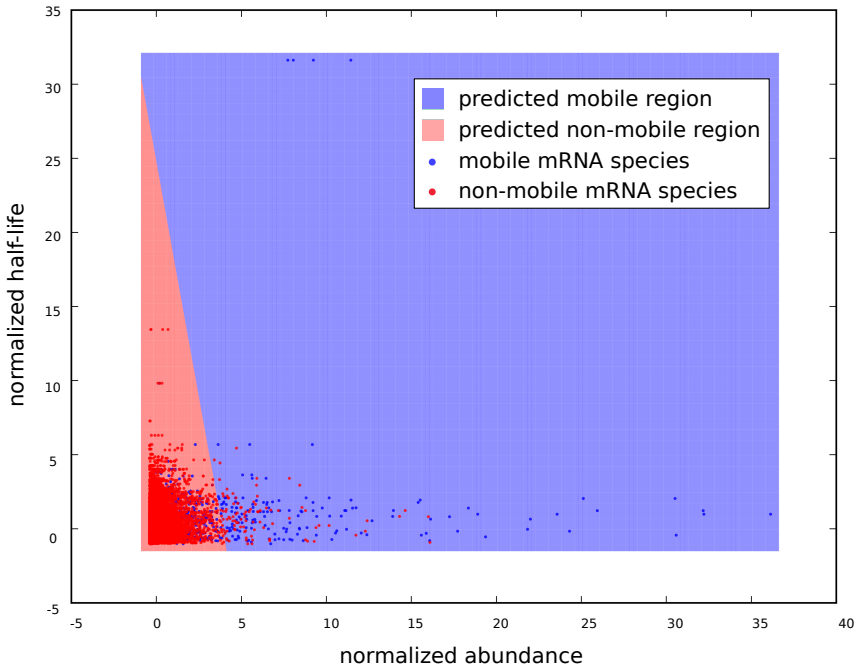


**Supplemental Figure 6: The contributions of half-life and abundance to mRNA mobility.** The relationship between experimental half-life, abundance and mRNA species mobility is shown, and the predicted regions of mobility, and non-mobility, generated using a logistic regression classifier. Abundance and half-life were both normalized such that the mean value is 0 and standard deviation is 1. The boundary between the predicted regions has separable abundance and half-life components.

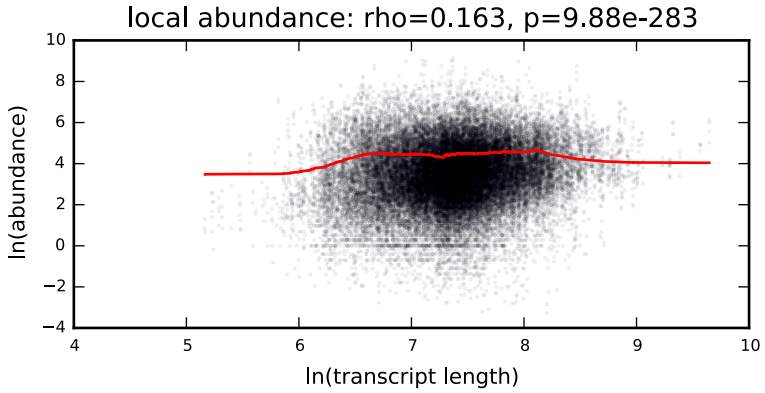


**Supplemental Figure 7: Detected transcript abundance as a function of length in the producing tissues.** A small but statistically significant positive correlation indicates that there is a slight detection bias favoring longer mRNA transcript. Data taken from Thieme et al. (2015), rho and p-values were calculated using Spearman's rank. The moving average (red) was calculated using a window size of 6000.

**Supplemental Table 1: List of low abundance mobile transcripts present in the data set of** Thieme et al. (2015)**.** To define low abundance we took a threshold based on Figure 2A, ln(abundance) < 1.

| Transcript ID | Gene Symbol | Gene Model Description |
|---|---|---|
| AT1G16160.1 | WALL ASSOCIATED KINASE-LIKE 5 (WAKL5) | WAK-like kinase |
| AT1G21250.1 | CELL WALL-ASSOCIATED KINASE (WAK1) | cell wall-associated kinase, may function as a signaling receptor of extracellular matrix component such as oligogalacturonides |
| AT1G32060.1 | PHOSPHORIBULOKINASE (PRK) | phosphoribulokinase (PRK) |
| AT1G42970.1 | GLYCERALDEHYDE-3-PHOSPHATE DEHYDROGENASE B SUBUNIT (GAPB) | chloroplast localized glyceraldehyde-3-phosphate dehydrogenase |
| AT1G52000.1 | | Mannose-binding lectin superfamily protein |
| AT1G52400.1 | BETA GLUCOSIDASE 18 (BGLU18) | member of glycosyl hydrolase family 1, located in inducible ER bodies, required in inducible ER body formation |
| AT1G56510.1 | WHITE RUST RESISTANCE 4 (WRR4) | TIR-NB-LRR protein that confers resistance to four races of Albugo candida |
| AT1G61520.1 | PHOTOSYSTEM I LIGHT HARVESTING COMPLEX GENE 3 (LHCA3) | PSI type III chlorophyll a/b-binding protein (Lhca3*1) |
| AT1G61610.1 | | S-locus lectin protein kinase family protein |
| AT1G65800.1 | RECEPTOR KINASE 2 (RK2) | encodes a putative receptor-like serine/threonine protein kinases that is similar to brassica self-incompatibility (S) locus |
| AT1G69730.1 | | Wall-associated kinase family protein |
| AT1G75920.1 | | GDSL-like Lipase/Acylhydrolase superfamily protein |
| AT2G35370.1 | GLYCINE DECARBOXYLASE COMPLEX H (GDCH) | Encodes glycine decarboxylase complex H protein |
| AT2G44840.1 | ETHYLENE-RESPONSIVE ELEMENT BINDING FACTOR 13 (ERF13) | encodes a member of the ERF (ethylene response factor) subfamily B-3 of ERF/AP2 transcription factor family |
| AT3G02620.1 | | Plant stearoyl-acyl-carrier-protein desaturase family protein |
| AT3G08940.2 | LIGHT HARVESTING COMPLEX PHOTOSYSTEM II (LHCB4.2) | Lhcb4.2 protein involved in the light harvesting complex of photosystem II |
| AT3G22121.1 | | Potential natural antisense gene, locus overlaps with AT3G22120 |
| AT3G26610.1 | | Pectin lyase-like superfamily protein |
| AT3G44860.1 | FARNESOIC ACID CARBOXYL-O-METHYLTRANSFERASE (FAMT) | Encodes a farnesoic acid carboxyl-O-methyltransferase |
| AT3G46780.1 | PLASTID TRANSCRIPTIONALLY ACTIVE 16 (PTAC16) | plastid transcriptionally active 16 (PTAC16) |
| AT3G49110.1 | PEROXIDASE CA (PRXCA) | Class III peroxidase Perx33 |
| AT3G50300.1 | | HXXXD-type acyl-transferase family protein |
| AT3G55800.1 | SEDOHEPTULOSE-BISPHOSPHATASE (SBPASE) | Encodes the chloroplast enzyme sedoheptulose-1,7-bisphosphatase (SBPase), involved in the carbon reduction of the Calvin cycle |
| AT3G61270.1 | | best Arabidopsis thaliana protein match is: |

| | | |
|---|---|---|
| | | downstream target of AGL15 2 (TAIR:AT2G45830.1) |
| AT4G11000.1 | | Ankyrin repeat family protein |
| AT4G13130.1 | | Cysteine/Histidine-rich C1 domain family protein |
| AT4G13620.1 | | encodes a member of the DREB subfamily A-6 of ERF/AP2 transcription factor family |
| AT4G14630.1 | GERMIN-LIKE PROTEIN 9 (GLP9) | germin-like protein with N-terminal signal sequence that may target it to the vacuole, plasma membrane and/or outside the cell |
| AT4G15160.1 | | Bifunctional inhibitor/lipid-transfer protein/seed storage 2S albumin superfamily protein |
| AT4G19170.1 | NINE-CIS-EPOXYCAROTENOID DIOXYGENASE 4 (NCED4) | chloroplast-targeted member of a family of enzymes similar to nine-cis-epoxycarotenoid dioxygenase |
| AT4G23150.1 | CYSTEINE-RICH RLK (RECEPTOR-LIKE PROTEIN KINASE) 7 (CRK7) | Encodes a cysteine-rich receptor-like protein kinase |
| AT4G26050.1 | PLANT INTRACELLULAR RAS GROUP-RELATED LRR 8 (PIRL8) | Encodes PIRL8, a member of the Plant Intracellular Ras-group-related LRRs (Leucine rich repeat proteins) |
| AT4G27440.1 | PROTOCHLOROPHYLLIDE OXIDOREDUCTASE B (PORB) | light-dependent NADPH:protochlorophyllide oxidoreductase B |
| AT4G29690.1 | | Alkaline-phosphatase-like family protein |
| AT4G31100.1 | | wall-associated kinase, putative |
| AT4G31354.1 | | This gene encodes a small protein and has either evidence of transcription or purifying selection |
| AT4G33610.1 | | glycine-rich protein |
| AT4G37220.1 | | Cold acclimation protein WCOR413 family |
| AT5G14650.1 | | Pectin lyase-like superfamily protein |
| AT5G25130.1 | CYTOCHROME P450, FAMILY 71, SUBFAMILY B, POLYPEPTIDE 12 (CYP71B12) | putative cytochrome P450 |
| AT5G25980.2 | GLUCOSIDE GLUCOHYDROLASE 2 (TGG2) | Myrosinase (thioglucoside glucohydrolase) gene involved in glucosinoloate metabolism |
| AT5G26260.1 | | TRAF-like family protein |
| AT5G26280.1 | | TRAF-like family protein |
| AT5G28500.1 | | unknown protein |
| AT5G38980.1 | | unknown protein |
| AT5G44580.1 | | unknown protein |
| AT5G46330.1 | FLAGELLIN-SENSITIVE 2 (FLS2) | leucine-rich repeat serine/threonine protein kinase that is expressed ubiquitously |
| AT5G55930.1 | OLIGOPEPTIDE TRANSPORTER 1 (OPT1) | oligopeptide transporter |
| AT5G60760.1 | | P-loop containing nucleoside triphosphate hydrolases superfamily protein |

**Supplemental Table 2: List of putative motifs identified in the low abundance mobile transcripts.** The motifs were enriched in the mobile vs. non-mobile low abundance transcripts. See Supplemental Table 1 for the list of transcripts. Data from Thieme et al. (2015).

| Enriched Motif | E-value | P-value |
|---|---|---|
| AGTWCAAC | 2.8e-2 | 7.6e-7 |
| ATGGTTTG | 3.2e-2 | 8.7e-7 |
| CCCACS | 4.7e-2 | 1.3e-6 |